EUROMECH Colloquium 511 on Biomechanics of Human Motion
J. Ambrósio et.al. (eds.)
Ponta Delgada, Azores, Portugal, March 9-12, 2011

A SIMPLE APPROACH TO ESTIMATE MUSCLE FORCES AND ORTHOSIS ACTUATION IN POWERED ASSISTED WALKING OF SPINAL CORD-INJURED SUBJECTS

J. Alonso[1], F. Romero[1], R. Pàmies-Vilà[2], U. Lugrís[3] and J.M. Font-Llagunes[2]

[1] Universidad de Extremadura
Avda. de Elvas s/n, 06006 Badajoz, Spain
e-mail: fjas@unex.es

[2] Universidad Politécnica de Cataluña
Av. Diagonal 647, 08028 Barcelona, Spain
{rosa.pamies, josep.m.font}@upc.edu

[3] Universidad de La Coruña
Mendizábal s/n, 15403 Ferrol, Spain
ulugris@udc.es

Keywords: Spinal cord injuries, Active orthoses, Musculoskeletal modeling, Optimization, Inverse Dynamics.

Abstract. *Simulation of walking in individuals with incomplete spinal cord injuries (SCI) wearing an active orthosis is a challenging problem from both the analytical and the computational points of view, due to the redundant nature of the simultaneous actuation of the two systems. The objective of this work is to quantify the contributions of muscles and active orthosis to the net joint torques, so as to assist the design of active orthoses for SCI. The functional innervated muscles of SCI patients were modeled as Hill-type actuators, while the idle muscles were represented by stiff and dissipative elements. The orthosis was included as a set of external torques added to the ankles, knees and hips to obtain net joint torque patterns similar to those of normal unassisted walking. The muscle-orthosis redundant actuator problem was solved through a physiological static optimization approach, for which several cost functions and various sets of innervated muscles were compared.*

1 INTRODUCTION

Spinal cord injuries cause paralysis of the lower limb extremities as they break the connections from the nervous central system to the muscles of the lower body. Incomplete spinal cord-injured (SCI) subjects can perform a low-speed, high-cost pathological gait by using walking aids such as crutches, canes or parallel bars. The energy cost and aesthetics of this walk can be improved by means of active orthoses, which require external actuation mechanisms to control the motion of the leg joints during the stance and swing phases of gait. To guide the development of active orthoses for SCI subjects, it is necessary to understand how the patient musculoskeletal actuation interacts with powered assistance to obtain a normal gait pattern. Considerable effort has been focused on the design and application of passive and active orthoses to assist standing and walking of SCI individuals, nevertheless, few studies [1-6] examine the moment joint patterns of combined patient-orthosis systems.

The first controllable active orthosis that can be found is a patent from 1942 of a hydraulically-actuated device for adding power at the hip and knee joints [7]. The first exoskeletons were developed at the University of Belgrade in the 60's and 70's to aid people with paraplegia resulting from spinal cord injury [7-8]. These early devices were limited to predefined motions and had limited success. However, new laboratory and commercially available rehabilitation devices and active orthoses designs have emerged in the last ten years. The proposed active orthotic devices add or dissipate power at their joints and/or release energy stored in springs during appropriate phases of gait [9]. These systems use in general a predefined motion pattern or moment joint pattern, qualitative and heuristic rules, classical control techniques or EMG-based control, but ignore the interaction between the human musculoskeletal system and the active orthosis. Moreover, the number of studies testing these systems on handicapped subjects is paradoxically low when compared with the studies on able-bodied subjects wearing the orthosis.

For example, the "Locomat" uses a predefined motion strategy to train muscles and nerve pathways for patients with locomotion impairment [10]. The "RoboKnee" is a powered knee brace developed by MIT that functions in parallel to the wearer's knee and transfers load to the wearer's ankle [11]. "HAL" is an orthosis developed by the University of Tsukuba in Japan that is connected to the patient's thighs and shanks, and provides a motion to its legs that is a function of the measured EMG signals [12-13]. The MIT Biomechatronics Lab developed a powered ankle-foot orthosis to assist drop-foot gait [14]: it consists of a modified passive ankle-foot orthosis with the addition of a series elastic actuator (SEA) to allow for variation in the impedance of flexion/extension motion of the ankle; the control of this device is based on ground contact force measurement and angle position data. Other approaches include the excitation of SCI muscles through the application of functional neuromuscular stimulation (FNS) [5,15]. However, excitation in FNS only systems can lead to instability, poor control, and limited walking distances due to muscle fatigue [5,15].

To assist the proper design of active orthoses for incomplete SCI, it is necessary to quantify the simultaneous contributions of muscles and active orthosis to the net joint torques of the human-orthosis system. Simulation of walking in individuals with incomplete SCI wearing an active orthosis is a challenging problem from both the analytical and the computational points of view, due to the redundant nature of the simultaneous actuation of the two systems. In this work, the functional innervated muscles of SCI patients were modeled as Hill-type actuators, while the idle muscles were represented by stiff and dissipative elements. The orthosis was included as a set of external torques added to the ankles, knees and hips to obtain net joint torque patterns similar to those of normal unassisted walking [2-3]. Kao et al. [2-3] suggest that able-bodied subjects aim for similar joint moment patterns when walking with and with-

out robotic assistance rather than similar kinematic patterns. The fundamental hypothesis of this work is that the combined actuation of the musculoskeletal system of the SCI subject and the active orthosis produce net joint moment patterns similar to those of normal unassisted walking. The muscle-orthosis redundant actuator problem was solved through a physiological static optimization approach, for which several cost functions and various sets of innervated muscles were compared.

2 BIOMECHANICAL MODEL

The biomechanical model used has 14 degrees of freedom. It consists of twelve rigid bodies linked with revolute joints (figure 1), and it is constrained to move in the sagittal plane. Each rigid body is characterized by mass, length, moment of inertia about the centre of mass, and distance from the centre of mass to the proximal joint.

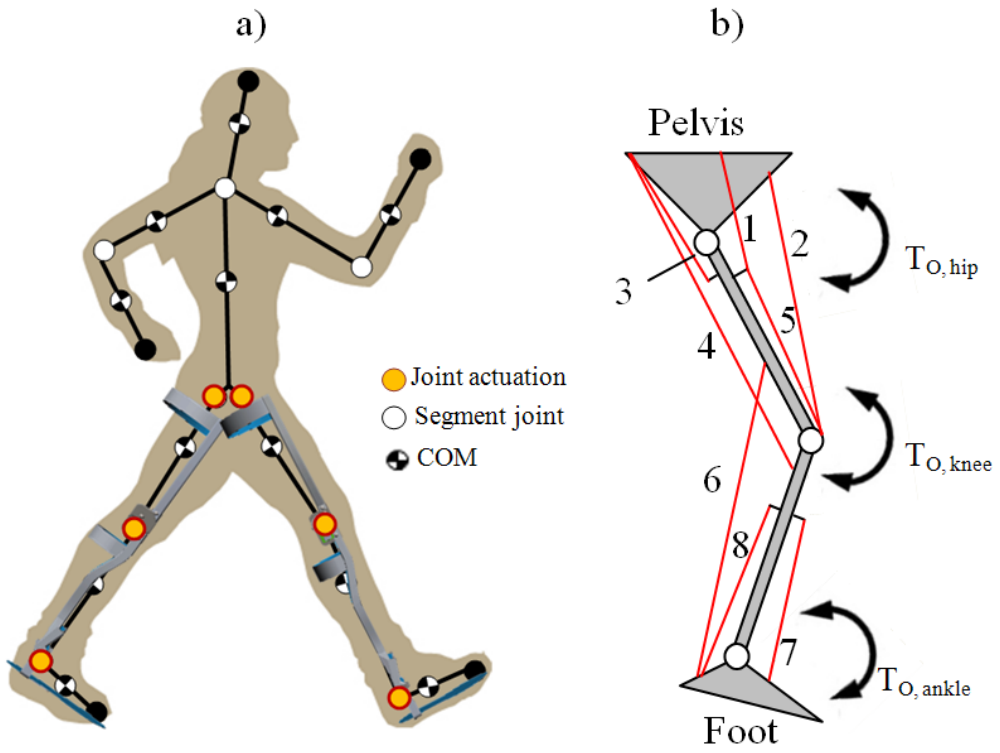

Figure 1: a) Planar biomechanical model of the human-orthosis system. b) Muscle groups: 1 – Iliopsoas, 2 – Rectus Femoris, 3 – Glutei, 4 – Hamstrings, 5 – Vasti, 6 – Gastrocnemius, 7 − Tibialis Anterior, 8 – Soleus.

The equations of motion can be written as:

$$\mathbf{M}\ddot{\mathbf{q}} + \mathbf{\Phi}_{\mathbf{q}}^{T}\boldsymbol{\lambda} = \mathbf{Q} \tag{1}$$

where $\mathbf{M}$ is the global (human-orthosis) mass matrix, $\mathbf{\Phi}_{\mathbf{q}}$ is the Jacobian matrix of the constraint equations, $\ddot{\mathbf{q}}$ is the acceleration vector, $\mathbf{Q}$ is the generalized force vector and $\boldsymbol{\lambda}$ are the Lagrange multipliers. Using kinematic and anthropometric data in equation (1), the net joint reaction forces and net driver (human-orthosis actuation) moments during a physical activity or motion and the ground reaction forces can be calculated. In order to quantify the simultaneous contributions of muscles and active orthosis to the net joint torques of the human-orthosis system, eight muscle groups and three external torques added to the ankles, knees and hips were considered in this analysis (shown in Fig. 1b).

The proposed external actuation is an active hip-knee-ankle-foot orthosis (A-HKAFO) to provide hip, knee and ankle joint moments to assist the pathological gait of SCI subjects.

2.1 Muscle model: innervated muscles

The functional innervated muscles of SCI patients were modeled as Hill-type actuators. Zajac [16] presented in 1989 the widely known Hill-type muscle-tendon model [17], which is shown in figures 2a) and 2b). The model consists of a contractile element (CE) that generates the force, a nonlinear parallel elastic element (PE), representing the stiffness of the structures in parallel with muscle fibers, and a nonlinear series elastic (SE) element that represents the stiffness of the tendon which is serially attached to the muscle and completes the musculotendon unit.

The two differential equations that govern the muscle dynamics are:

$$\dot{a} = h(u, a) \tag{2}$$

$$\dot{f}_{mt} = g(l_{mt}, \dot{l}_{mt}, a, f_{mt}) \tag{3}$$

The first equation is the activation dynamics equation that relates muscle excitation u from the central nervous system (CNS) and muscle activation a. Equation (3) defines the force-generation properties as a function of force–fiber length l_{mt} and force–fiber velocity $\dot{l}_{mt}$ relationships. In this work the activation dynamics was not considered.

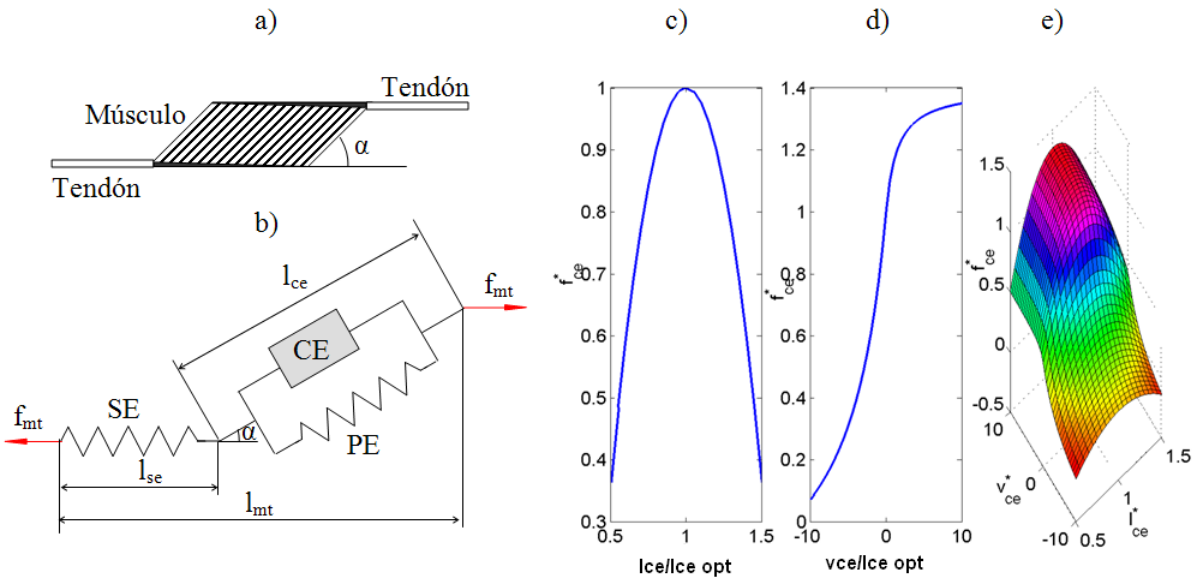

Figure 2: Muscle model for innervated muscles. a) Conceptual scheme. b) Hill model [16]. c) Normalized force-length relation model. d) Normalized force-velocity relation model. e) Force-length-velocity model.

The force generated by the CE, f_{ce} is a function of the activation a, its length l_{ce}, and its contraction velocity v_{ce}. These relationships are shown in figures 2c and 2d. If the pennation angle α is constant, according to figure 2b:

$$l_{mt} = l_{se} + l_{ce}\cos\alpha \tag{4}$$

$$f_{mt} = f_{se} = (f_{ce} + f_{pe})\cos\alpha \approx f_{ce}\cos\alpha \tag{5}$$

where the force of the parallel elastic element PE is set to zero [18-22]. The tendon (SE) can be modeled by a simple quadratic force-strain curve:

$$f_{se} = f_{mt} = \begin{cases} 0 & si \quad l_{se} < l_{ts} \\ k_t \left(l_{se} - l_{ts} \right)^2 & si \quad l_{se} > l_{ts} \end{cases} \tag{6}$$

where l_{ts} is the tendon slack length and k_t is the SE stiffness:

$$k_t = \frac{f_0}{\left(\varepsilon_0 l_{ts} \right)^2} \tag{7}$$

ε_0 (3% to 5%) is the strain occurring at the maximal isometric muscle force f_0, see Winters [23]. The force-length relationship for CE (figure 2c) is:

$$f_{ce} = f_0 \left[1 - \left(\frac{l_{ce} - l_{ce}^{\ opt}}{w} \right)^2 \right] \tag{8}$$

where $l_{ce}^{\ opt}$ is the muscle fibers optimal length and the width parameter w can be found in [19, 23]. Finally, force-velocity expression for a concentric contraction $v_{ce} < 0$ (figure 2d) reads as:

$$\frac{f_{ce}}{f_0} = a \cdot \frac{B_r \left(f_{iso} + A_r \right) - A_r \left(B_r - \dfrac{\dot{l}_{ce}^{\ N}}{f_{ac}} \right)}{B_r - \dfrac{\dot{l}_{ce}^{\ N}}{f_{ac}}} \tag{9}$$

where $\dot{l}_{ce}^{\ N} = \dot{l}_{ce} / l_{ce}^{\ opt}$, $A_r = 0.41$, $B_r = 5.2$, and $f_{iso} = f_{iso}(w, l_{ce}^{\ opt}, l_{ce})$ is the muscle isometric force relative to the maximal isometric muscle force f_0 and $f_{ac} = \min(1, 3.33a)$. A detailed description of equation (9) can be found in [19]. The values for the adopted parameters are shown in table 1 obtained from [19]. Using equations (1-6) the overall model contraction dynamics equation can be expressed as the nonlinear first-order differential equation (3) [18-22].

	$l_{ce}^{\ opt}$ (m)	w	f_0 (N)	l_{ts} (m)	α (º)	l_{m0} (m)	r_a (m)	r_k (m)	r_h (m)
Psoas	0.102	1.298	821	0.142	7.5	0.248	0	0	−0.050
RF	0.081	1.443	663	0.398	5.0	0.474	0	0.050	−0.034
Glu	0.200	0.625	1705	0.157	3.0	0.271	0	0	0.062
BF	0.104	1.197	1770	0.334	7.5	0.383	0	−0.034	0.072
Vas	0.093	0.627	7403	0.223	4.4	0.271	0	0.043	0
Gas	0.055	0.888	1639	0.420	14.3	0.404	0.053	−0.020	0
TA	0.082	0.442	1528	0.317	6.0	0.464	−0.037	0	0
Sol	0.055	1.039	3883	0.245	23.6	0.201	0.053	0	0

Table 1: Muscle parameters.

2.2 Denervated muscles

Injury to the human spinal cord typically results in paralysis of muscles innervated by spinal segments at or below the trauma. Denervated muscles show features of denervation atrophy and weakness [24] whose severity depends on the time elapsed from the injury. Atrophy of these paralyzed muscles is common but the magnitude of the weakness has rarely been evaluated. In [3,24] the strength of a SCI injured subject's denervated and innervated muscles is reported to vary between 4% and 97% [24].

The AIS (ASIA Impairment Scale) grade indicates the severity of the injury from A (complete) to E (normal motor and sensory functions). In the C and D cases, the motor function is preserved below the neurological level (lowest segment where motor and sensory functions are normal), being the difference between C and D the muscle activity grading.

Nevertheless, the AIS grade has one drawback: muscle scores are poor predictors of intrinsic muscle strength, for example muscles graded as having normal strength are often considerably weaker than the muscles of able-bodied subjects [24].

On the other hand, the atrophy of denervated muscles increases the passive moments at the joints, which include the moments generated by all other passive structures crossing the joints, like ligaments, too. Several studies [25-26] show that passive torque tended to be larger in the pathological than in the healthy participants, nevertheless the changes in passive stiffness and viscous damping associated to different pathologies seem to be inconsistent [25-26].

In this work the muscle weakness is modeled limiting the maximum activation of denervated muscle by a weakness factor $p \subset [0,1]$ that limits the maximum muscle activation. The contraction dynamics for a denervated muscle is:

$$\dot{f}_{mt} = g(l_{mt}, \dot{l}_{mt}, p \cdot a, f_{mt}) \tag{10}$$

To model the increment of passive torque due to muscle atrophy, stiff and dissipative elements were added to joints, namely, a linear damping and nonlinear stiffness, which were estimated from experimental data of SCI subjects, were added to the knee and ankle joints, and their values were the approximate average values obtained by pendulum experiments performed [25-26]. The values of stiffness and viscous damping are chosen to be 2.6798 Nm/rad^2 based on [25] and 0.8647 Nms/rad based on [26].

The calculation of the passive torque due to muscle atrophy is important to determine the torque needs of the active orthotic device to assist gait. Figure 3 shows the increment of the ankle and knee moments due to pathological passive torque compared with the moments in normal gait (obtained for a benchmark described in Section 4). The results show slight differences except for the knee flexion-extension during swing phase (0-0.35 seconds). Assuming that the hip muscles are fully innervated in incomplete SCI subjects, no additional passive torque was added to hip joint [24].

3 OPTIMIZATION APPROACH

Since several muscles serve each joint of the skeletal system, muscle forces cannot be directly computed from joint moments. This is the well-known redundant actuator problem in biomechanics. In order to solve this problem, optimization procedures are used. Several optimization methods (static optimization, dynamic optimization, augmented static optimization, large-scale static optimization) and optimization criteria (minimum metabolical cost of transport, minimum sum of muscle stresses, minimum hyper-extension of the joints, time-integral cost of activations, torque-tracking) are available in the literature [27-41]. The optimization assumes that the load sharing between the muscles follows certain rules during learned motor activities and muscle recruitment strategy is governed by physiologic criteria that achieve

functional efficiency. In this work, the muscle-orthosis redundant actuator problem was solved through a physiological static optimization approach.

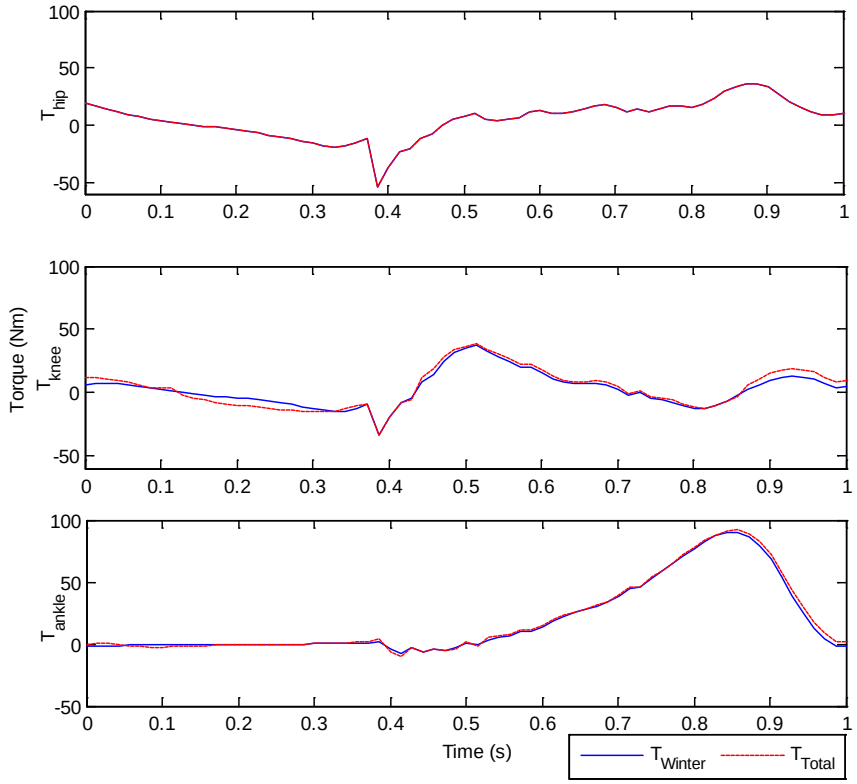

Figure 3: Hip, knee and ankle moments during normal gait (continuous line) and pathological gait (dashed line).

3.1 Static optimization

The inverse dynamics based static optimization methods are known for three decades. In a first step, net joint torques are calculated using the inverse dynamics approach. The muscular load sharing problem is then solved for each instant in time by minimizing a cost function $J(\mathbf{F}_{mt})$ depending on muscle forces (for example sum of muscle tensions). This optimization problem is subject to the constraint that the sum of muscle moments must equals the net joint torque obtained by inverse dynamics [28].

In the pathological gait of incomplete SCI subjects, the active orthosis should complement the disabled subject's musculoskeletal system so as to provide the efforts required to achieve a motion close to that of normal walking. The load sharing optimization problem for the combined orthosis-SCI subject actuation can be formulated as follows:

$$\begin{aligned} &Min \quad && J(\mathbf{F}_{mt}, \mathbf{T}_o) \\ &s.t. \quad && \mathbf{R} \cdot \mathbf{F} = \mathbf{T} \\ & && 0 \le \mathbf{F}_{mt} \le \mathbf{p} \cdot \mathbf{F}_0 \\ & && -\mathbf{T}_o^{*} \le \mathbf{T}_o \le \mathbf{T}_o^{*} \end{aligned} \tag{11}$$

where $\mathbf{F} = [\mathbf{F}_{mt}, \mathbf{T}_o]^T = [f_{mt,1}, \ldots, f_{mt,N}, T_{o1}, T_{o2}, T_{o3}]^T$ is the muscular and orthosis actuation vector at each instant, N is the number of muscle groups, $\mathbf{R}$ is the constant matrix of equivalent moment arms of the different muscle groups and orthosis actuators and $\mathbf{T}$ is the vector of net

joint torques obtained from inverse dynamics analysis considering the dissipative effects of denervated muscles at ankle and knee joints. Moment arms are defined as the distance between the muscle line of action and the joint axis of rotation. The muscle lengths and moment arms can be determined as functions of the generalized coordinates using expressions or tables available in the literature (see, for example, Menegaldo et al. [33]). The moment arms of each muscle with respect to ankle r_a, knee r_k and hip r_h are shown in table 1.

The second constraint implies that the maximum possible muscular forces are limited by its maximum isometric force $p_i f_{0,i}$, where $\mathbf{F}_0 = \left[f_{0,1},\ldots, f_{0,N}\right]^T$. The third constraint ensures that the orthosis actuation does not exceed the maximum torque available $\mathbf{T}_0^*$.

Two families of cost functions were proposed [7-10]:

$$J_1(\mathbf{F}_{mt}, \mathbf{T}_o) = \omega_{mt} \sum_{j=1}^{N} \left(\frac{f_{mt,j}}{C_j} \right)^n + \omega_o \sum_{k=1}^{3} \left(\frac{T_{o,k}}{T_{o,k}^*} \right)^n \tag{12}$$

$$J_2(\mathbf{F}_{mt}, \mathbf{T}_o) = \omega_{mt} \sum_{j=1}^{N} \left(- f_{ce,j} v_{ce,j} \right)^n + \omega_o \sum_{k=1}^{3} \left(T_{o,k} \dot{\theta}_k \right)^n \tag{13}$$

where N is the number of muscle groups, $f_{mt,j}$ is the force of muscle unit j and C_j is its physiologic cross-sectional area (PCSA). $T_{o,k}$ is the external torque provided by the orthosis at joint k, $\dot{\theta}_k$ is the angular velocity at joint k, $n = 2$ and ω_{mt}, ω_o are the weighting factors assigned to muscular and orthotic actuations respectively. The first cost function minimizes the weighted sum of muscle stresses raised to the *n*th power and the sum of the orthosis utilization factors at each joint raised to the *n*th power. Equation (12) is not dimensionally consistent, so ω_o must be high enough to balance the weights of muscle stresses and orthosis actuation. The second function minimizes the weighted sum of muscle work rate to the *n*th power and work rate of orthosis actuation.

Static optimization (SO) is computationally efficient compared to dynamic optimization since it does not require multiple integrations of the equations of motion. Nevertheless, this procedure does not consider the excitation and contraction dynamics of the muscle, which can lead to physiological inconsistent results. To overcome this drawback, a simple physiological static optimization approach is proposed in this work.

3.2 Physiological static optimization

A modified version of the classical static optimization approach that takes into account muscle physiology is proposed in this section. This scheme considers the muscle contraction dynamics, ensuring the physiological consistency of the obtained solution and being efficient from a computational point of view compared to dynamic optimization approaches.

The proposed optimization approach comprises two steps: in the first step, the inverse contraction dynamics problem is solved, assuming that muscle activations are maxima. The second step calculates the activations compatible with the net joint torques obtained by inverse dynamics using a static optimization approach.

In the first step, the length and velocity of each musculotendon unit l_{mt}, $\dot{l}_{mt}$ are obtained from generalized coordinates of the multibody model and the initial musculotendon lengths l_{m0} (table 1). Then, the maximum muscle force histories $f_{mt}^*(t)$ compatible with contraction

dynamics are calculated supposing that the muscle activation are maxima at every instant $\mathbf{A}_m = [a_1, \ldots, a_N]^T = [1, \ldots, 1]^T$. Briefly, for each muscle, the contraction dynamics differential equation is integrated:

$$\frac{df_{mt}^{\ *}}{dt} = g((a = 1) \cdot p,\ f_{mt}^{\ *}, l_{mt}, \dot{l}_{mt}) \tag{14}$$

In the second step, the muscle activations and orthosis actuation is calculated solving the optimization problem:

$$\begin{aligned} \textit{Min} \qquad & J_1(\mathbf{A}_m, \mathbf{A}_o) = \omega_{mt} \sum_{j=1}^{N} \left(\frac{a_j f^{*}_{mt,j}}{C_j} \right)^2 + \omega_o \sum_{k=1}^{3} \left(\frac{o_k T_{o,k}}{T_{o,k}^{\ *}} \right)^n \\ \textit{s.t.} \qquad & \mathbf{R} \cdot \left(\mathbf{AF}^{*} \right) = \mathbf{T} \\ & 0 \le a_j \le 1 \\ & -1 \le o_k \le 1 \end{aligned} \tag{15}$$

where $\mathbf{AF}_{mt}^{\ *} = \left[a_1 \cdot p_1 \cdot f_{mt,1}^{\ *}, \ldots, a_N \cdot p_N \cdot f_{mt,N}^{\ *}, o_1 \cdot T_{o,1}^{\ *}, o_2 \cdot T_{o,2}^{\ *}, o_3 \cdot T_{o,3}^{\ *} \right]^T$. The variables o_k ensure that the orthosis actuation does not exceed the maximum available actuator torque at joint *k*. In order to compare the results of statics and physiological static optimization, the function:

$$J_2(\mathbf{F}_{mt}, \mathbf{T}_o) = \omega_{mt} \sum_{j=1}^{N} \left(- f_{ce,j} v_{ce,j} \right)^n + \omega_o \sum_{k=1}^{3} \left(T_{o,k} \dot{\theta}_k \right)^n \tag{16}$$

was also minimized using the physiological static optimization (PSO) approach.

4 RESULTS AND DISCUSSION

The static and physiological static approaches (equations 11-13 and 15-16 respectively) were applied to calculate muscle forces and orthosis actuation during walking in order to assist the pathological gait. In the adopted procedure, normal gait motion data is used as input to the biomechanical model. Namely, the 2D walking kinematic Benchmark data from Winter [35] was used to perform an inverse dynamic analysis. The acquired movement is a normal cadence non-pathological gait stride, carried out by a healthy female subject with 57.75 kg of weight. The analysis comprises a period of 1 s. The kinematic data was acquired using a sampling frequency of 70Hz. The obtained net driver ankle and knee moments were corrected to consider the dissipative effects of muscle atrophy in SCI subjects (Figure 3).

The optimization problems were solved using the MATLAB^{TM} gradient-based routine "fmincon" implemented in the Optimization Toolbox that uses a sequential quadratic programming (SQP) method. Two different sets of innervated muscles were compared in order to compare the results for an AIS C and AIS D SCI subject. According to ASIA Impairment Scale:

- AIS C: Motor function is preserved below the neurological level, and more than half of key muscles below the neurological level have a muscle grade less than 3. In this case, the innervated and denervated muscles were defined by the vector $\mathbf{p} = [1, 0.2, 1, 0.2, 0.2, 0.2, 0.2, 0.2]^T$. See figure 1b for muscle description.
- AIS D: Motor function is preserved below the neurological level, and at least half of key muscles below the neurological level have a muscle grade of 3 or more. In

this case, the innervated and denervated muscles were represented by the vector $\mathbf{p} = [1,1,1,1,0.4,0.4,0.4,0.4]^T$.

Figures 4, 5 and 6 represent the muscle and orthosis actuation obtained using the static and physiological static approaches for AIS C and AIS D subjects.

The results using static and physiological static optimization were similar, according to results obtained by other authors [30] due to low contraction velocities for gait, except for the Soleus and Tibialis anterior muscles. The weightings factors for cost function J_1 were $\omega_{mt} = 1$ and $\omega_o = 10^{10}$ and for cost function J_2 were $\omega_{mt} = 1$ and $\omega_o = 1.5 \cdot 10^{-4}$. Results show that a proper designed HKAFO can assist the pathological gait cycle of both AIS C and D incomplete SCI subjects to approach normal kinetic gait patterns at joints.

The orthosis actuation prevents stance phase knee flexion due to quadriceps weakness, assists swing-phase knee flexion-extension and corrects insufficient ankle plantarflexor torque to achieve normal moment patterns at the hip, knee and ankle joints during gait.

The examination of figures 4-6 reveals that the torque needs of the active orthotic device are similar to the ones developed by the human ankle, knee and hip joints. The calculated maximum required torque for the orthosis is about 30 Nm at the hip and 20 Nm at the knee for both AIS C subjects and AIS D subjects. During stance phase, the orthosis modulates the plantarflexor torque according to injury severity AIS C or AIS D. The needed external actuation at the ankle is 65 Nm for AIS C subjects and about 40 Nm for AIS D subjects. The obtained results were comparable to that obtained using control approaches [3].

Note that the obtained results must be interpreted with caution, since the muscle weakness coefficient p_1 must be evaluated in real SCI subjects. Moreover, the weight of the orthosis has been neglected and this mass would increase the required moments at the hip and knee joints, especially at hip and knee during swing phase as reported by other authors [1].

Regarding the computational cost of each formulation, the CPU mean time was 10.29 s for the static optimization approach. To solve the physiologic static optimization problem, first, the contraction equation (14) was integrated using the Euler method (CPU time 0.42 s) and the optimization problems (15) and (16) were solved in a mean time of 9.04 s. The initial guess for the two approaches (SO and PSO) was zero. The results show that the computational cost of the proposed approach is low compared with other physiological static formulations proposed [19-22, 33].

5 CONCLUSIONS

This work presents a simple and efficient approach to estimate muscle forces and orthosis actuation in powered assisted walking of incomplete spinal cord-injured subjects. The proposed scheme is computationally efficient and ensures the physiological consistency of the obtained results. The major contribution of the optimization approach is that the contraction dynamics equation is integrated in a first step to obtain the maximum physiologic available muscle forces. The final objective is to develop a computer application that enables to virtually test different types of active orthoses for gait assistance on disabled subjects suffering from spinal cord injury and other gait pathologies. The results of this application are the efforts of the disabled subject, along with the orthosis forces required to produce the desired normal kinetic gait patterns at joints. The obtained results seem to be promising, nevertheless to attain the final objective much work has to be done in several topics:

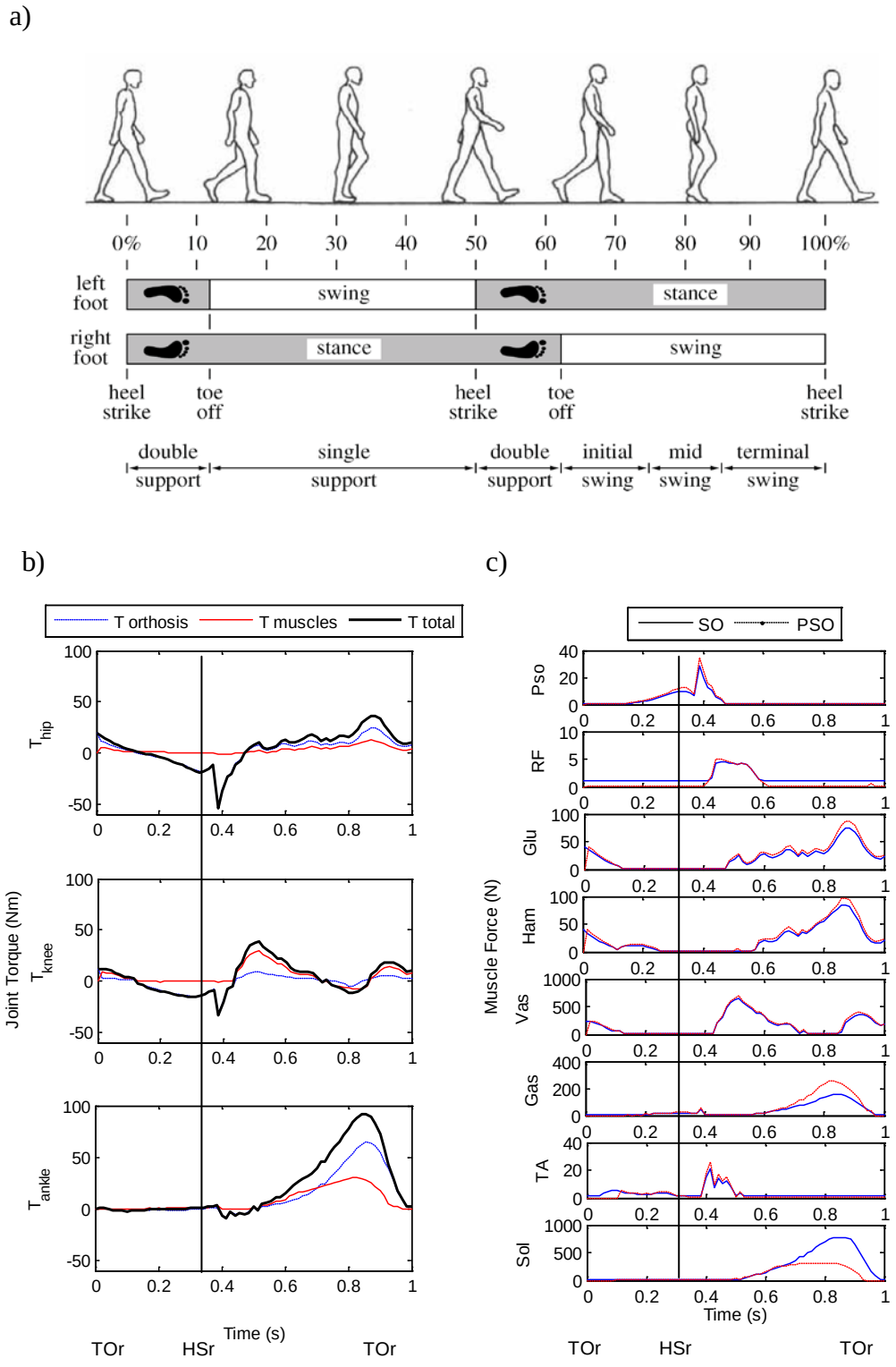

Figure 4: Results. a) Human gait phases. Source: [19]. b) Joint torques for an ASIA C subject obtained by PSO and using cost function J_1. c) Muscular forces for an ASIA C subject obtained by SO and PSO and using cost function J_1. TOr, right toe off.; HSr, right heel strike. Vertical continuous line separates swing and stance phases.

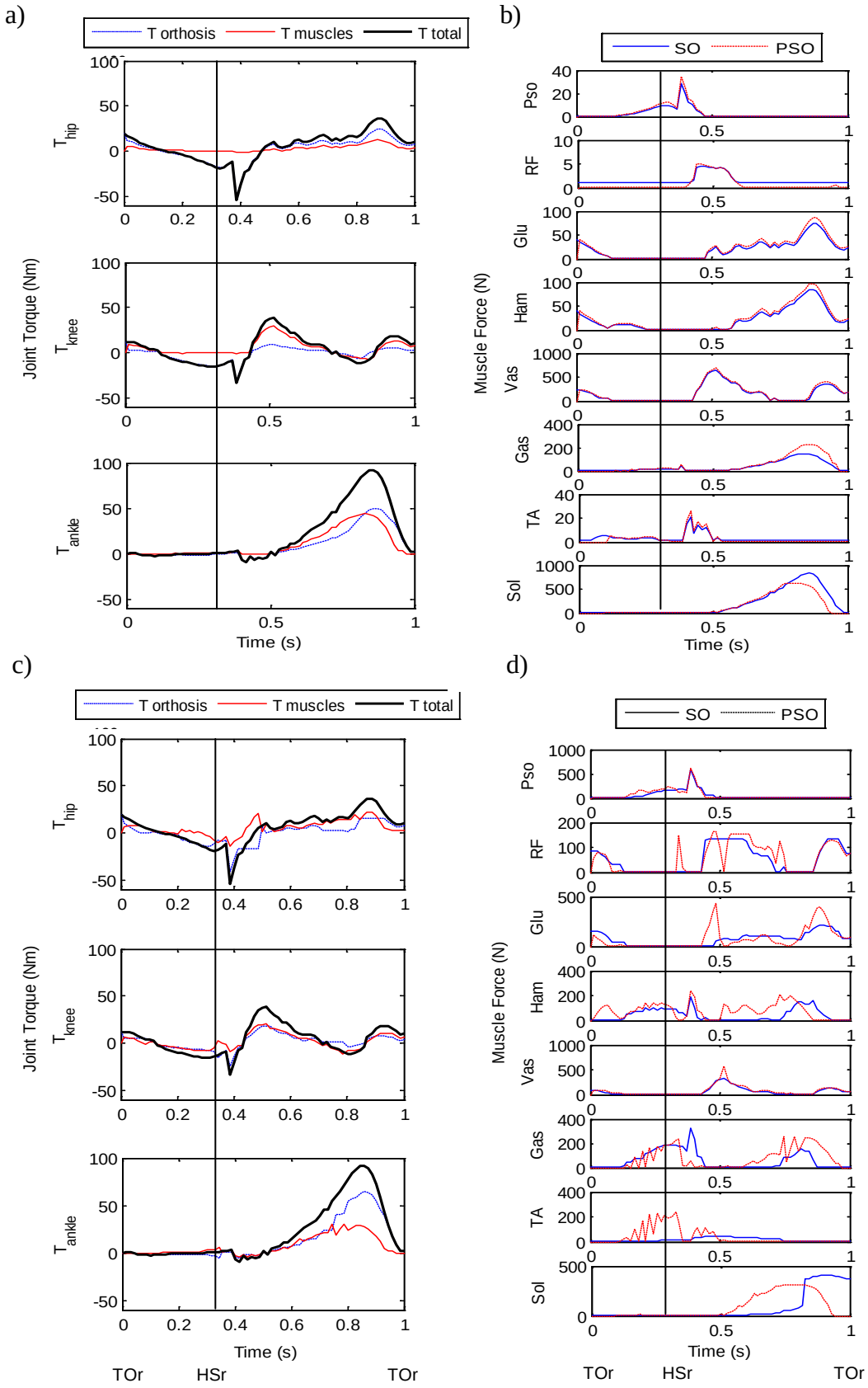

Figure 5: a) Joint torques for an ASIA C subject obtained by PSO and using cost function J_2. b) Muscular forces for an ASIA C subject obtained by SO and PSO and using cost function J_2. c) Joint torques for an ASIA D subject obtained by PSO and using cost function J_1. d) Muscular forces for an ASIA C subject obtained by SO and PSO and using cost function J_1. TOr, right toe off.; HSr, right heel strike.

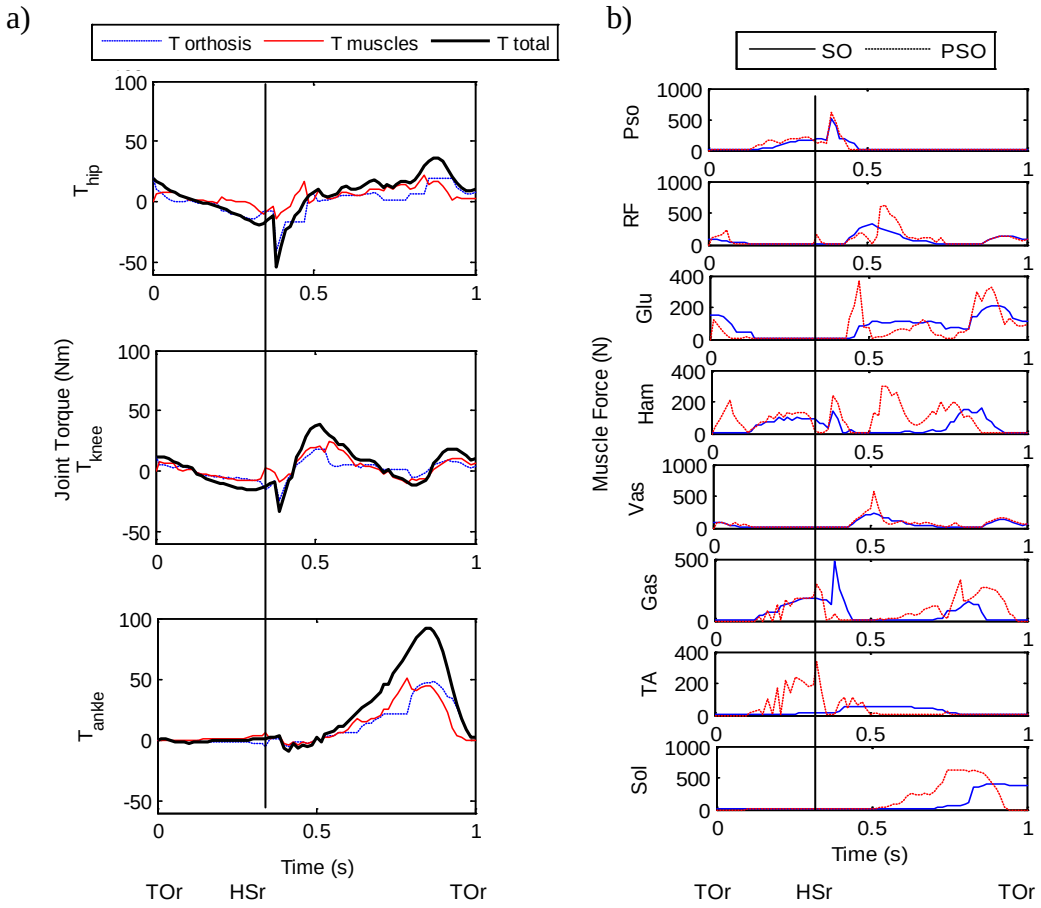

Figure 6: a) Joint torques for an ASIA D subject obtained by PSO and using cost function J_2. b) Muscular forces for an ASIA C subject obtained by SO and PSO and using cost function J_2. TOr, right toe off.; HSr, right heel strike.

- Include in the optimization problem the contact loads transmitted at the leg-orthosis interface in order to obtain contact pressures below the PPTs (Pain Pressure Thresholds), which represent the patient's comfort.

- The optimization cost function adopted for disabled-bodied subjects will be revised since disability may affect it.

- The way in which the disability affects the subject will have to be deeply investigated in order to make the corresponding changes in the model of able-bodied subject so as to obtain a model of disabled subject. Namely, the force-generation dynamics and the parameters of the impaired muscle and passive torque due to muscle atrophy will be adapted according to the results available in the literature for the considered disability. Such a model will undergo then a validation procedure.

- The obtained results must be compared with forward dynamics optimization and parametric schemes. In this case, the desired motion of the disabled subject wearing the

active orthosis, namely a scaled-normalized able-bodied gait pattern, should be first defined. The forward dynamics module should consider the combined actuation of the musculoskeletal system and the active orthosis and validate the hypothesis of net joint moment invariance.

- A walking aid mimicking canes and voluntary upper extremity actions to maintain lateral stability by providing the necessary shoulder forces and moments must be included in the inverse or forward dynamic simulations in order to obtain more realistic results.

6 ACKNOWLEDGMENT

This work is supported by the Spanish Ministry of Science and Innovation under the project DPI2009-13438-C03. The support is gratefully acknowledged.

REFERENCES

[1] P. C. Silva, M. T. Silva and J. M. Martins, Evaluation of the Contact Forces Developed in the Lower Limb/Orthosis Interface for Comfort Design, Multibody System Dynamics, **24**, 367-388, 2010.

[2] P.C. Kao, C.L. Lewis, and D.P. Ferris, Invariant Ankle Moment Patterns when Walking with and without a Robotic Ankle Exoskeleton, *Journal of Biomechanics*, **43**, 203-209, 2010.

[3] P.C. Kao, C.L. Lewis, and D.P. Ferris, Joint Kinetic Response during Unexpectedly Reduced Plantar Flexor Torque Provided by a Robotic Ankle Exoskeleton during Walking, *Journal of Biomechanics*, **43**, 1401-1407, 2010.

[4] Pons, J.L., *Wearable robots: biomechatronic exoskeletons*. Wiley Blackwell, 2008.

[5] C. S. To, R. F. Kirsch, R. Kobetic and R. J. Triolo, Simulation of a Functional Neuromuscular Stimulation Powered Mechanical Gait Orthosis with Coordinated Joint Locking, *IEEE Transactions on Neural Systems and Rehabilitation Engineering*, **13**(2), 227-235, 2005.

[6] S.K. Agrawal and A. Fattah, Theory and Design of an Orthotic Device for Full or Partial Gravity-Balancing of a Human Leg During Motion. *IEEE Transactions on Neural Systems and Rehabilitation Engineering*, **12**(2), 157-165, 2004.

[7] M. Vukobratovic, V. Ciric and D. Hristic, Contribution to the Study of Active Exoskeletons, *Proceedings of the 5th IFAC Congress*, Paris, France, 1972.

[8] M. Vukobratovic, D. Hristic and Z. Stojiljkovic, Development of Active Anthropomorphic Exoskeleton, *Medical & Biological Engineering & Computing*, **12**, 66-80, 1974.

[9] A.M. Dollar, H. Herr, Active Orthoses for the Lower-Limbs: Challenges and State of the Art, *Proceedings of the 2007 IEEE 10th International Conference on Rehabilitation Robotics*, Noordwijk, The Netherlands, 968-977, 2007.

[10] G. Colombo, M. Jorg and V. Dietz, Driven Gait Orthosis To do Locomotor Training of Paraplegic Patients, *22nd Annual International Conference of the IEEE-EMBS*, Chicago, USA, 2000.

[11] J. Pratt, B. Krupp, C. Morse and S. Collins, The RoboKnee: An Exoskeleton for Enhancing Strength and Endurance During Walking, *IEEE Int. Conference on Robotics and Automation*, New Orleans, USA, 2004.

[12] H. Kawamoto, S. Kanbe and Y. Sankai, Power Assist Method for HAL-3 Estimating Operator's Intention Based on Motion Information, *Proceedings of 2003 IEEE Workshop on Robot and Human Interactive Communication*, Millbrae, CA, IEEE, New York, 67-72, 2003.

[13] H. Kawamoto and Y. Sankai, Power Assist System HAL-3 for gait Disorder Person, *ICCHP*, Austria, 2002.

[14] J.A. Blaya and H. Herr, Adaptive Control of a Variable-Impedance Ankle-Foot Orthosis to Assist Drop-Foot Gait, *IEEE Transactions on Neural Systems and Rehabilitation Engineering*, **12**, 24-31, 2004.

[15] G. T. Yamaguchi and F. E. Zajac, Restoring Unassited Natural Gait to Paraplegics Via Functional Neuromuscular Stimulation: A Computer Simulation Study, *IEEE Transactions on Biomedical Engineering*, **37** (9), 1990.

[16] F. Zajac, Muscle and Tendon: Properties, Models, Scaling and Applications to Biomechanics and Motor Control. *Crit. Rev. Biomed. Eng.*, **17**, 359-411, 1989.

[17] A. Hill, The Heat of Shortening and the Dynamic Constants of Muscle. *Proc. R. Soc. London Ser. B*, **126**, 136-195, 1938.

[18] M. Ackermann and W. Schiehlen, Dynamic Analysis of Human Gait Disorder and Metabolical Cost Estimation, *Arch. Appl. Mech.*, **75**, 569-594, 2006.

[19] M. Ackermann, *Dynamics and energetics of walking with prostheses*, Ph.D. thesis, University of Stuttgart, Stuttgart, 2007.

[20] S. E. Rodrigo, J. A. C. Ambrósio, M. P. T. Silva and O. H. Penisi, Analysis of Human Gait Based on Multibody Formulations and Optimization Tools, *Mechanics Based Design of Structures and Machines*, **36**, 446-477, 2008.

[21] D. García and W. Schiehlen. Simulation of Human Walking With One-Sided Gait Disorders. *Proceedings of the 1st Joint International Conference on Multibody System Dynamics*. 1st Joint International Conference on Multybody System Dynamics (1). Num. 1. Lapperanta, Finland, 2010.

[22] J. Winters, *Concepts in neuromuscular modeling, three-dimensional analysis of human movement*, Human Kinetics Publishers, Champaign, IL, 1995.

[23] C.K. Thomas and R. M. Grumbles, Muscle Atrophy after Human Spinal Cord Injury, *Biocybernetics and Biomedical Engineering*, **25**(3), 39-46, 2005.

[24] M. F. McDonald, M. K. Garrison and B. D. Schmit, Length–Tension Properties of Ankle Muscles in Chronic Human Spinal Cord Injury, *Journal of Biomechanics*, **38**, 2344-2353, 2005.

[25] M. K. Lebiedowska and J. R. Fisk, Passive Dynamics of the Knee Joint in Healthy Children and Children Affected by Spastic Paresis, *Clinical Biomechanics*, **14**(9), 653-660, 1999.

[26] B.M. Nigg and W. Herzog (Eds.), *Biomechanics of the musculo-skeletal system*, 2nd ed., Wiley, 1999.

[27] R. Crowninshield and R. A. Brand, A physiologically based criterion of muscle force prediction in locomotion, *Journal of Biomechanics*, **14**, 793-801, 1981.

[28] G.T. Yamaguchi, D.W. Moran and J. Si, A Computationally Efficient Method for Solving the Redundant Problem in Biomechanics, *Journal of Biomechanics*, **28**, 999-1005, 1995.

[29] F.C. Anderson and M.G. Pandy, Static and Dynamic Optimization Solutions for Gait are Practically Equivalent, *Journal of Biomechanics*, **34**, 153-161, 2001.

[30] C. Rengifo, Y. Aoustin, F. Plestan and C. Chevallereu, Distribution of Forces between Synergistics and Antogonistics Muscles using an Optimization Criterion depending on Muscle Contraction Behaviour. *Journal of Biomechanical Engineering*, **132**, 1-11, 2010.

[31] F.C. Anderson and M.G. Pandy, Dynamic Optimization of Human Walking, *Journal of Biomechanical Engineering*, **123**, 381-390, 2001.

[32] L.L. Menegaldo, A.T. Fleury and H.I. Weber, A 'Cheap' Optimal Control Approach to Estimate Muscles Forces in Musculoskeletal Systems, *Journal of Biomechanics*, **39** 1787-1795, 2006.

[33] D.G. Thelen and F.C. Anderson, Using Computed Muscle Control to Generate Forward Dynamic Simulations of Human Walking from Experimental Data, *Journal of Biomechanics*, **39**, 321-328, 2006.

[34] G. Pipeleers, B. Demeulenaere, I. Jonkers, P. Spaepen, G. Van der Perre, A. Spaepen, J. Swevers and J. De Schutter, Dynamic Simulation of Human Motion: Numerically Efficient Inclusion of Muscle Physiology by Convex Optimization, *Optimization Engineering*, **9**, 213-238, 2008.

[35] D.A. Winter, *Biomechanics and motor control of human gait: normal, elderly and pathological*, 2nd ed., University of Waterloo Press, Waterloo. Ontario, 1991.

[36] J. Ambrosio and A. Kecskemethy, Multibody Dynamics of Biomechanical Models for Human Motion via Optimization, In: *Multibody Dynamics Computacional Methods and Applications* (J.C. Garcia Orden, J.M. Goicolea and J. Cuadrado, eds.), Springer, 2007.

[37] D. Tsirakos, V. Baltzopoulos and R. Barlett, Inverse Optimization: Functional and Physiological Considerations Related to the Force-Sharing Problem, *Critical Reviews in Biomedical Engineering*, **25**, 371-407, 1997.

[38] H. Hatze, Neuromusculoskeletal Control Systems Modeling: A Critical Survey of Recent Developments, *IEEE Transactions on Automatic Control*, **25**, 375-385, 1980.

[39] H.J. Ralston, *Energetics of human walking, neural control of locomotion*, Plenum Press, New York, 1976.

[40] F. Anderson and M. Pandy, Static and Dynamic Optimization Solutions for Gait are Practically Equivalent, *Journal of Biomechanics*, **34**, 153-161, 2001.

[41] H. Hatze, The Fundamental Problem of Myoskeletal Inverse Dynamics and its Implications, *Journal of Biomechanics*, **35**, 109-115, 2002.